

VPSI 2.0: IoT-Based Hybrid Protocol With Simultaneous Equations for Real-Time Seizure Classification and False-Negative Mitigation

Karthikeyan Gopalakrishnan^{ID}, Arunkumar Balakrishnan^{ID}, Kousalya Govardhanan, and Kandala N. V. P. S. Rajesh

Abstract—Nonepileptic seizures are a clinical symptom of abnormally high synchronous cortical activity known as psychogenic nonepileptic seizures (PNESs) as they exhibit no outward signs of neurological damage. The need for differentiating PNES from full-body general seizures (GTCSs) decreases therapy time and ensures proper hospice. Internet of Medical Things (IoMT) provide a closed-loop mechanism to accurately measure seizures. The erratic nature of seizures has drawn the attention where false detection could have catastrophic impact. This article discusses the vibration profile seizure identifier (VPSI) 2.0 where vibration profile analysis of an ictal patient is measured in real-time to classify seizures in an IoMT framework. The novel seizure detection model has been proposed for differentiating between multiple seizure types. The simultaneous equation (S.E) protocol is developed for noninvasive stigma-free monitoring of seizures for continual monitoring. S.E-based Internet of Things (IoT) seizure classifier is helpful to mitigate challenges present in detecting real-time occurrences of seizure by 95.683% in a controlled environment.

Index Terms—Generalized tonic-clonic seizure (GTCS), Internet of Medical Things (IoMT), Internet of Things (IoT), psychogenic nonepileptic seizure (PNES), seizures.

I. INTRODUCTION

P SYCHOGENIC nonepileptic seizures (PNESs) mimic epileptic seizures but do not involve aberrant electrical discharges in the brain. These episodes might cause tonic or clonic limb movements. Sexually or physically abused people, especially adult women, are more likely to acquire PNES. Few PNES patients obtain the necessary information to control seizures without psychological trauma. The interplay between these risk factors that cause ictal episodes is unknown. Depression, anxiety, post-traumatic stress disorder, and psychological difficulties may occur as adverse effects.

Received 6 August 2024; revised 3 October 2024; accepted 22 October 2024. Date of publication 28 October 2024; date of current version 21 February 2025. (Corresponding author: Arunkumar Balakrishnan.)

Karthikeyan Gopalakrishnan is with the Department of Computer Science and Engineering, Coimbatore Institute of Technology, Coimbatore 641014, India (e-mail: karthikeyan.g@cit.edu.in).

Arunkumar Balakrishnan is with Department of Information Technology, Manipal Institute of Technology Bengaluru, Manipal Academy of Higher Education, Manipal, India (e-mail: arunkumar.b@manipal.edu).

Kousalya Govardhanan is with the Department of Computer Science and Engineering, Dayananda Sagar University, Bengaluru 560078, India (e-mail: kousalya-cse@dsu.edu.in).

Kandala N. V. P. S. Rajesh is with SENSE, VIT-AP, Amaravathi 522237, India (e-mail: rajesh.k@vitap.ac.in).

Digital Object Identifier 10.1109/JIOT.2024.3486991

Thus, an intelligent healthcare solution is needed to improve seizure detection and management, reducing long-term issues. The research provides an intelligent sensor prototype for epileptic seizure detection. These sensors can detect seizures by replicating them on a prosthesis.

PNESs are misdiagnosed as status epilepticus 8.1% of the time, making treatment difficult. At a rate of 20.1%, adolescents and young adults had the highest relative occurrence. Poor diagnosis of PNES patients can lead to respiratory depression and inappropriate intubation, which occurred in 26% of cases of anti-seizure medicine maladministration. In 33% of patients, adjunctive pharmacotherapy causes nonresponsiveness and significant adverse effects. This emphasizes the importance of precise diagnosis and individualized treatment [1].

The detection of seizures encompasses a range of techniques, such as clinical observation conducted by healthcare experts, electroencephalography (EEG), video-EEG monitoring, ambulatory EEG, diagnostic imaging, seizure diaries, and seizure alarms. However, these methods have drawbacks. EEG and imaging are limited by cost and availability. Invasive monitoring is risky and not always necessary. Different detection methods are sensitive to seizures, which could potentially miss subtle manifestations. External factors, including patient adherence and subjective seizure diary and clinician observation can also cause diagnostic changes and ambiguity. Patients feel even more ostracized because many detecting tools tend to be inappropriate for public wear. Existing seizure detection systems, including EEG caps, large-scale monitoring devices, and wrist-worn sensors, are often highly visible and intrusive, which may exacerbate the social stigma faced by patients when used in public settings. These tools can draw unwanted attention, leading to feelings of self-consciousness and social ostracization. To address this issue, the proposed wearable technology aims to be discreet and seamlessly integrated into everyday clothing or accessories, thereby reducing the visibility of the device and helping patients feel more comfortable and less stigmatized in public settings.

This study seeks to address these challenges by developing a compact, unobtrusive device for ictal monitoring and seizure classification. The system enables continuous monitoring and accurate seizure detection without disrupting patients' daily activities. Utilizing advanced sensor technologies and real-time data processing algorithms, the wearable device offers discreet, noninvasive seizure detection and classification. Unlike

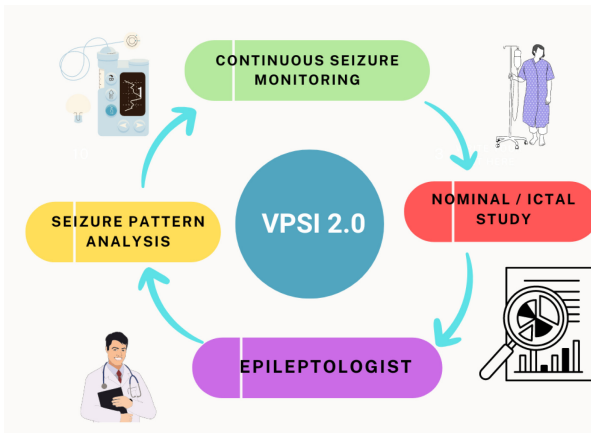


Fig. 1. Closed loop solution of epilepsy monitoring.

traditional monitoring methods, such as cumbersome EEG systems or manual recordings by caregivers, these smart-watches are inconspicuous and integrate effortlessly into daily life. Historically, individuals with epilepsy have experienced social stigmatization stemming from misunderstandings and misconceptions about the condition. The presence of visible monitoring devices or the necessity for constant supervision can intensify feelings of being different or singled out, potentially leading to social isolation or discrimination. Additionally, the noninvasive nature of this technology eliminates the need for uncomfortable attachments or intrusive procedures, making the monitoring process more comfortable and less distressing for patients. This level of discretion significantly reduces the visibility of the medical condition, thereby minimizing the stigma often associated with epilepsy and other seizure disorders. The device's portability and simplicity provide patients more autonomy and trust in managing their medical condition, improving their quality of life.

By integrating seizure detection sensors with intelligent categorization and identification algorithms, the efficiency and accuracy of identifying appropriate hospice care protocols can be significantly enhanced. Seizure monitors measure periodic vibration profiles to track preictal, postictal, and ictal states [2], [3], [4], [5]. The neurologist can develop an appropriate course of treatment for an individual with epilepsy, whether they experience psychogenic nonepileptic seizures (PNESs) or generalized seizures. The Internet of Things (IoT) closed-loop monitoring system uses S.E. technology to detect seizures. Refer to Fig. 1. The suggested seizure monitoring system is an IoT-integrated system for nonclinical seizure observation. It would make classifying sporadic and unpredictable seizures easier to reduce their impact.

A. Preliminaries and Background

Currently, patients with seizures often face a significant loss of independence due to the unpredictable onset of their episodes. This study examines an IoT-based vagus nerve stimulation (VNS) system designed to deliver calibrated electrical impulses to the vagus nerve via the jugular region, providing targeted therapeutic intervention. The detection mechanism was limited by to detecting generalized tonic-clonic seizure

TABLE I
LIST OF ACRONYMS AND TERMS

Acronym	Definition
GTCS	Generalized Tonic-Clonic Seizures
NES	Non-Epileptic Seizure
PNES	Psychogenic Non-Epileptic Seizure
VPSI 2.0	Vibration Profile Seizure Identifier
S.E.	Simultaneous Equation
EEG	Electroencephalography
SUDEP	Sudden Unexpected Death In Epilepsy
FDA	Food And Drug Administration
Ictal	The Phase During Which A Seizure Occurs
Preictal	The Phase Before A Seizure Begins
Postictal	The Phase Following The End Of A Seizure

(GTCS) seizure by studying the pulse and blood circulation parameters. If the patient is suffering from a localized seizure the system under study will be ignorant of the difference. Thus, for patients with PNES to benefit from therapies like VNS or in general to have a quicker and clearer understanding of the type of seizures encountered by patients a system with demarcation prerogatives for accurate classification is mandatory. The proposed system utilizes the seizure protocols of GTCS and trained protocols for PNES for accurate classification.

B. Acronyms and Terms

To facilitate a clear understanding of the terminology and abbreviations used throughout this article, we provide a comprehensive list of acronyms and terms in Table I. This section includes definitions for key terms related to seizure disorders, diagnostic methods, and treatment approaches, ensuring that readers can easily reference and comprehend the concepts discussed in the following sections. The table below outlines these terms and their meanings.

C. Our Vision: Precise IoMT Seizure Classification: VPSI 2.0

During ictal and preictal stages, monitoring indicators like blood pressure (B.P.), heart rate, and bodily motions can help control epilepsy. This enables proper control. Consult [6]. Epileptics with unexpected seizures must recognize and identify seizures. The patient's EEG is monitored in real time during ictal stages. Neurologist understands and advises on seizure prevention. However, EEG is not a practical method for nonclinical monitoring in real time. B.P., heart rate, and vibration patterns are thus examined as an alternative biomarker. Continuous monitoring could improve epilepsy care with the data. Refer to Fig. 2 for our Internet of Medical Things (IoMT)-based seizure classification concept.

vibration profile seizure identifier (VPSI) 2.0 is a noninvasive, wearable intelligent biomarker observation device with a continuous seizure classifier. This classifier uses a body vibration sensing method [7]. It expands on our previous article, "GTCS-Vagus Nerve Stimulator Automation Using Private IoT-Blockchain Smartcontract." It addresses electrical therapy for grand-mal seizures with security measures. Training data from an 18-year-old Brazilian patient with myoclonic GTCSs were utilized to construct the seizure classifier. Normal and ictal seizure patterns were analyzed

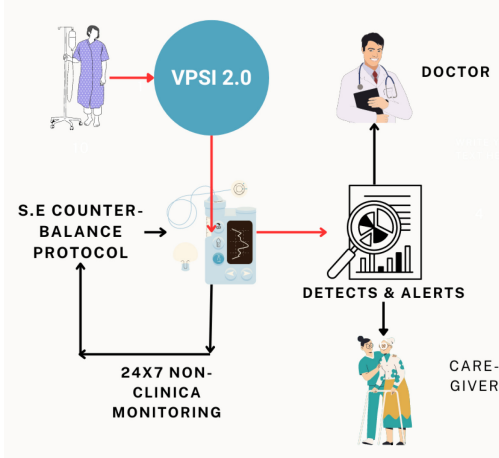


Fig. 2. Stakeholder communication flow of closed loop solution.

using this data [8]. Seizures are categorized using vibration characteristics in this study. The wearable classification system VPSI 2.0 confronts many challenges, including: 1) patients' seizure patterns fluctuate; 2) sensor selection and response for seizure detection; and 3) identifying seizure types without false-negatives throughout preictal and ictal stages.

While the classifier was trained using data from a single 18-year-old Brazilian patient with myoclonic GTCSs, the consistent features of GTCS—such as generalized spike-and-wave discharges and rhythmic muscle contractions—support the applicability of this dataset. The classifier's generalizability is reinforced by rigorous validation, including cross-validation techniques, which ensure its reliability. Clinical experts have affirmed that the dataset accurately reflects typical GTCS presentations. Although expanding the dataset remains a challenge, the scalable methodology employed allows for future integration of diverse data to further validate and refine the model. The model has demonstrated robust effectiveness in distinguishing GTCS from normalcy to detect PNES, with several factors ensuring its scalability. Seizure types often exhibit overlapping physiological markers, such as EEG patterns and autonomic responses, which allow the model to generalize across diverse seizure presentations. Rigorous cross-validation strengthens its reliability, while the simultaneous equation (S.E) framework ensures adaptability by integrating features specific to other seizures. Incorporating insights from absence and focal seizures, further expanding the S.Es can achieve broader generalizability and scalability across all seizure types.

A seizure classifier for epileptic patients' erratic movements has been developed. This classifier detects preictal and ictal epilepsy using vibration oscillations, B.P. spikes, and heart rate fluctuations. Patient seizures, such as GTCS (Grand-Mal) or PNES, would be classified using the vibration model in the proposed seizure classifier. Citations include [9], [23]. The model would delineate seizures based on observed deviations in nominal and seizure states and BP and HR data. Nonclinical epilepsy monitoring can be done with the classifier to protect patients' privacy and minimize social shame. GTCS and PNESs can be accurately measured and analyzed with the technology. Preventing sudden unexpected death in epilepsy

(SUDEP) requires a clear plan and caregiver advice. Medical device categorization protocols in the IoT are essential for seizure diagnosis and treatment. The S.E approach improves PNES sensor detection of small patterns. S.E. optimizes the accuracy of detection by effectively counterbalancing error patterns identified in a patient's seizures, thereby eliminating the necessity for human intervention. This balancing is necessary because conventional sensors can only detect 38.2% of seizures (simulated). The objective of S.E. is to determine a solution that satisfies all equations simultaneously [23]. S.E is a set of two or more equations that involve multiple variables, where the goal is to find a common solution that satisfies all equations simultaneously [23]. The S.E solution is a simple and efficient approach that may be implemented with minimal specialized apparatus. Seizure classifiers use S.E protocols to improve closed loop epilepsy monitoring system precision and confidence.

This article's flow is as follows. Section II summarizes the main contribution and prior research. Section III discusses the S.E classification prosthetic model. The S.E model is explained in Section IV. Section V discusses the outcomes. Section VI concludes and outlines future directions.

II. PRIOR RESEARCH WORK AND NOVEL CONTRIBUTION

A. Related Work and Consumer Products

Smart healthcare is one of the most sought-after applications of IoT with an estimated 176 billion by 2026 [24]. IoT in healthcare has allowed physicians and caregivers an affordable avenue to treat patients continuously in a nonclinical environment. This technology allows patients, including those who may be unconscious or incapacitated by seizures, to receive timely and continuous care while managing their health conditions outside of traditional clinical settings. This advancement enhances both the convenience and accessibility of medical monitoring and intervention. Neuro-Detect presented a smart healthcare solution that combined EEG with a machine learning model [23], [23], [24]. The IoT framework was utilized to create an automated seizure recognition system, which employed DWT and DNN approaches. Similarly, the smart IoT-edge gateway for wellness care was designed to work with a variety of medical equipment [24]. A novel packet generation structure was created to address interoperability difficulties with healthcare sensors in consumer medical ecosystems. GTCS epilepsy monitor via smart watch heart rate monitoring was developed using Blockchain framework. The biomarker spike percentile was used to detect patterns in real time. For seizure management, specific seizure category-based monitoring was lacking due to the erratic nature of seizures. Continuous monitoring technology was sought to replace traditional observation techniques to maintain a round-the-clock situation report in epilepsy patients.

Commercial epilepsy monitoring devices are primarily EEG-based, such as "Epileptic-Seizure-Detection-Using-DWT-Based-Fuzzy-Approximate-Entropy-And-Support-Vector-Machine." However, they lack wearability, requiring patients to remain still, hindering daily monitoring and causing social stigma if openly disclosed [23], [23], [24], [24].

TABLE II
COMPARISON OF SEIZURE DETECTION RESEARCH WORKS

Research Works	Age	Gender	Strata	Caregiver	Support	Intensity	Psychiatric Status	QoL
Cioriceanu et al.	✓	✓	✗	✗	✗	✗	✗	✓
Saker et al. & Newmaster et al.	✗	✓	✗	✗	✗	✗	✓	✗
Doss et al. & T. Sawchuk et al.	✗	✗	✗	✗	✓	✗	✓	✓
P.J. Thompson et al. & I. Faiman et al. & C.C. Ogoke et al. & Qi et al.	✗	✗	✗	✗	✗	✓	✓	✓
E. Grillo et al.	✗	✗	✗	✓	✗	✗	✗	✗

Another FDA-approved device is the “Embrace” smart system, employing sensors like accelerometer, electrodermal activity, temperature, and gyroscope to record data and alert seizures, albeit without distinguishing among them [23], [23], [24]. Gammacore (nVNS—Vagus Nerve Stimulator) technology targets chronic headaches through VNS but lacks specificity in post-ictal therapy [24], [25]. Existing devices detect seizures but limited to specific types and require frequent patient-specific calibrations, lacking robust classification and 24 × 7 nonclinical assessment [26], [27], [28], [29], [30].

The parameters outlined in Table II provide a comprehensive framework for evaluating the multidimensional impact of seizures on both patients and caregivers, as commonly considered by epileptologists. Given these limitations, there is a pressing need for more advanced and user-friendly epilepsy monitoring solutions. Addressing these challenges, the current paper introduces a novel approach that significantly improves upon existing technologies.

B. Novel Contributions of the Current Paper

Building upon these insights, the current paper introduces an accurate noninvasive edge device, the GTCS-Vagus Nerve Stimulator Automation Using Private IoT-Blockchain Smartcontract. This device delivers electrical therapy to GTCS seizure patients securely and inexpensively. It is an IoT-integrated wearable gadget that uses instantaneous heart rate and pulse variation with Smartcontract for security. To reduce false positives (FPs), patient-specific seizure patterns were calibrated against an open-source seizure data set of an 18-year-old myoclonic GTCS epileptic patient. The current paper presents an accurate real-time seizure classification employing calibrated vibration protocols as VPSI 2.0, which provides IoMT-integrated continuous seizure monitoring. It presents a novel and reliable seizure classification approach for on-site diagnosis, incorporating a closed-loop control system to mitigate associated stigma. The need for a transparent and robust sensing technology as outlined by Qi et al., [31] is evident from the inferences of patient clinical and oral testimonies.

This article proposes the following major contributions.

- 1) Affordable counter-balanced closed-loop monitoring system.
- 2) VPSI 2.0 serves IoMT networks with a wearable, low-energy protocol. Mitigates stigma as it can be worn beneath clothes.
- 3) The IoMT-incorporated closed-loop system assesses HR, BP, and movement patterns to categorize seizures.

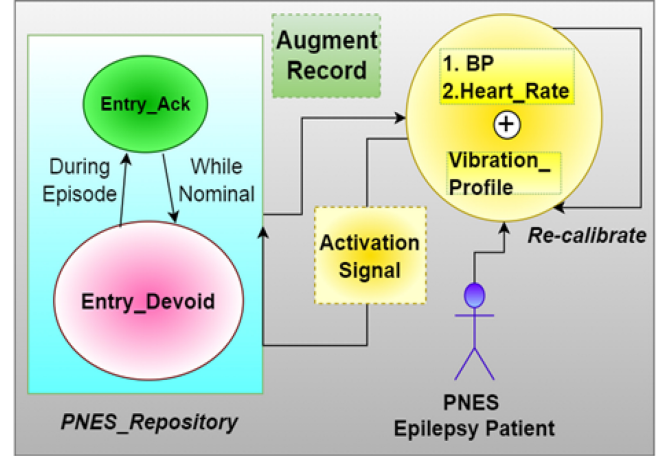


Fig. 3. Ictal vibration classifier with IoMT framework.

- 4) The system is caregiver-independent and uses a calibrated, low-cost counter-balance for accuracy.

III. PROPOSED SEIZURE CLASSIFIER: VPSI 2.0

The seizure model integrates with VPSI 2.0 to detect ictal vibrations in real time. Furthermore, the heart rate and B.P. are used to corroborate and validate the preictal and ictal findings. The ictal categorization system responds to biomarker stimuli, as seen in Fig. 3.

A. Closed Loop Ictal Classifier

The intelligent VPSI 2.0 ictal sensor at the carotid, ulnar, and radial nodes will continually monitor the epileptic patient. The ictal phase of a seizure causes erratic body movements at one node or throughout the body. Brain discharges that deviate from the expected course induce GTCS seizures in humans. Stress-related, psychological, or emotional displays may resemble epileptic convulsions. GTCS’s ictal phase affects the entire body, causing post-ictal coma. In contrast, PNES localizes ictal symptoms to one or more limbs while retaining consciousness. In preictal and ictal stages, B.P. and heart rate fluctuate greatly, although GTCS and PNES differ minimally. The distinctions in GTCS and PNES symptoms, together with B.P. and pulse rate, can assist delineate seizure types in such circumstances. Localized ictal episodes and biomarker spikes can indicate PNES, while a trigger of all three nodes and a drop in biomarkers due to LOC can indicate GTCS. Accurate seizure type detection necessitates effective noise elimination and minimization of false negatives (FNs), which are critical for improving nonclinical monitoring

and optimizing therapeutic recommendations. Nonetheless, the presence of FNs diminishes detection accuracy, making the application of counterbalance techniques essential.

B. Proposed Seizure Classification Model

A new seizure detection and classification model uses vibration patterns as the major classification parameter and mean arterial pressure (MAP) and B.P. as supplementary factors. The patient's wrist and neck's ulnar, carotid, and radial nodes determine the vibration pattern. Equations (1) and (2) define the PNES-GTCS difference equation

$$\text{PNES}_{\text{Id}}(R_w)^n = \sum_{n=0}^{\text{Test Cases}} \left(\int_{35}^{75} 0.025 \cdot \text{BP}(t) dt \{t, 35, 75\} - \int_{35}^{75} \text{GTCS}(t) dt \{t, 35, 75\} \right) \quad (1)$$

$$\text{PNES}_{\text{Id}}(L_w)^n = \sum_{n=0}^{\text{Test Cases}} \left(\int_{35}^{75} 0.025 \cdot \text{BP}(t) dt \{t, 35, 75\} - \int_{35}^{75} \text{GTCS}(t) dt \{t, 35, 75\} \right). \quad (2)$$

The system was calibrated against the B.P limit of (35, 75) to restrict detection to the nominal range of age considered, and non-PNES indicators were eliminated using a comparable range of verified GTCS seizures. This is to generate a close approximation of the myoclonic patient used as a reference. 0.025 is the first calibration offset to improve detection accuracy. Whereas $\text{PNES}_{\text{Id}}(L_w)^n$ and $\text{PNES}_{\text{Id}}(R_w)^n$ indicate the variation rate displayed in the ulnar and radial nodes, using GTCS parameters from the previous model as references to highlight differences. The two nodes will identify seizures alone during PNES, whereas all nodes experience GTCS

$$\text{PNES}_{\text{Id}}(N_k)^n = \sum_{n=0}^{\text{Test Cases}} \int_{35}^{75} 0.025 \cdot \text{BP}(t) dt \{t, 35, 75\}. \quad (3)$$

Whereas $\text{PNES}_{\text{Id}}(L_Wrist)^n$ is detected exclusively because both PNES and GTCS use the carotid nerve as an intermediate; (4) defines seizure range by active seizure rate change

$$\begin{aligned} \text{Range} &= [\text{PNES}_{\text{Id}}(R_w)^n - \text{PNES}_{\text{Id}}(L_w)^n] \\ &\text{ModBm}[V_p * \text{PNES}_{\text{Id}}(N_k)^n]. \end{aligned} \quad (4)$$

In (4), the "Range" [-0.025 to -0.075] rate measurement compares node statements and differentiates them to identify seizure type, where Bp, Hr, and Vp indicate node biomarkers. The modulus function is used to separate the influence of outliers observed on account of noise and unexpected volatility in ictal states

$$\text{Sez_Tpe} = \frac{\text{PNES}_{\text{Id}}(N_k)^n}{\text{Range} \cdot (\text{PNES}_{\text{Id}}(L_W) + R_W)^n}. \quad (5)$$

In (4), "Sez_Type" represents seizure type detection, using the carotid node as a reference for GTCS absence. Grand-mal seizures result in "ve" ranges, while PNES results in zero

TABLE III
IMPACT OF VARIABLES ON DETECTION ACCURACY

Variable	Impact Description
Metal Prostheses	Caused noise, leading to false readings.
Motion Artifacts	Distorted data due to movement.
Sensor Sensitivity	Affected accuracy due to sensitivity.
Environmental Noise	External interference disrupted signals.
Signal Interference	Interference from external sources.

ranges. The original system had a 38.5% detection accuracy due to sensor errors caused by noise, particularly from metal prostheses in the experimental study. These introduced false readings, especially in the vibration parameters, affecting detection reliability. Additional factors, refer Table III, such as motion artifacts, sensor sensitivity, environmental noise, and signal interference, also contributed to the inaccuracies.

To mitigate these issues, artificial calibration using S.E methods was applied to calculate counter-balance variables at each detection point, significantly reducing the impact of noise and improving the system's precision. This adjustment provided more reliable seizure detection across parameters.

C. S.E Protocol–Augmenting Vibration Accuracy

Individual SW-420 vibration sensors that monitor seizure patients' vibration patterns limit equation (5) via FNs. To offset inaccurate negative results, we build deliberate inaccuracies into the equation. Under simulated scenarios of GTCSs, PNESs, and normal states, equations show the proportion of successfully recognized seizures to the total number of seizures. The identification of PNES includes LPNES (the left wrist), RPNES (the right wrist), and NPNES (neck or jugular). SW-420 vibration sensors are labeled α (the left wrist), β (jugular), and γ (the right wrist) for S.Es.

S.E Hypothesis 1: Asymmetric Localized-Sensor

$$\begin{aligned} 0.5\alpha + 0.5\beta + 0.5\gamma &= 0.7 \quad \text{GTCS} \\ 1.3\alpha + 0.3\beta + 0.15\gamma &= 0.43 \quad \text{L_PNES} \\ 0.15\alpha + 0.3\beta + 1.3\gamma &= 0.47 \quad \text{R_PNES} \\ 0.3\alpha + 1.4\beta + 0.3\gamma &= 0.6 \quad \text{N_PNES} \\ \alpha + \beta + \gamma &= 1 \quad \text{Nominal.} \end{aligned} \quad (6)$$

S.E Hypothesis 2: Symmetric Localized-Sensor

$$\begin{aligned} 0.5\alpha + 0.5\beta + 0.5\gamma &= 0.7 \quad \text{GTCS} \\ \alpha + 0.5\beta + 0.25\gamma &= 0.43 \quad \text{L_PNES} \\ 0.25\alpha + 0.5\beta + \gamma &= 0.47 \quad \text{R_PNES} \\ 0.5\alpha + \beta + 0.5\gamma &= 0.6 \quad \text{N_PNES} \\ \alpha + \beta + \gamma &= 1 \quad \text{Nominal.} \end{aligned} \quad (7)$$

These systems of equations, upon balancing, yield a factor to counterbalance FNs from each wrist sensor. The Arduino Uno, despite its limited computational power, can efficiently solve a 5×5 system of linear equations, handling 125 cubic operations within milliseconds and utilizing 120 bytes of its 2 KB SRAM capacity. The use of precomputed values ($\alpha = 0.346$, $\beta = 0.274$, and $\gamma = 0.034$) significantly reduces computational complexity and ensures numerical stability. This approach not only enhances real-time processing but also

maintains minimal computational impact, making it a viable solution for accurate and efficient seizure detection in practical applications.

- 1) *S.E Hypothesis 1: Asymmetric Localized-Sensor Biased Counter-Balance Ratio Distribution:* Individual sensors at isolated seizure nodes are prioritized for seizure detection. The two ancillary sensors corroborate the seizure site sensors' detection percentile. GTCS is a grandmal seizure, an ictal phenomena experienced roughly uniformly across the patient's physiology, hence its equation is symmetrical. “ α , β , and γ ” indicate the vibration sensor values from the left wrist, jugular, and the right wrist, respectively

$$\begin{aligned} \text{Principal_equation} &= \sum(\text{GTCS} + \text{L_PNES} + \text{R_PNES} \\ &\quad + \text{N_PNES} + \text{Nominal}) \\ &= 3.25\alpha + 3.5\beta + 3.25\gamma = 3.2. \end{aligned} \quad (8)$$

- a) *Eliminating β :*

$$\begin{aligned} \text{L_PNES} - \text{R_PNES} : 1.3\alpha + 0.3\beta + 0.15\gamma &= 0.43 \\ - (0.15\alpha + 0.3\beta + 1.3\gamma) &= 0.47 \\ \text{Sub - equation (1)} : \gamma &= 0.034 + \alpha. \end{aligned} \quad (9)$$

- b) *Arriving α :*

$$\begin{aligned} \text{N_PNES} - \text{Nominal} : 0.3\alpha + 1.4\beta + 0.3\gamma &= 0.6 \\ - (1.4\alpha + 1.4\beta + 1.4\gamma) &= 1.4. \end{aligned}$$

$$\begin{aligned} \text{Replacing } \gamma &= 0.034 + \alpha \text{ in N_PNES - Nominal} \\ \alpha &= 0.346(\text{sol1}). \end{aligned} \quad (10)$$

- c) *Arriving γ via backpropagation of α in (1)*

$$\gamma = 0.034 + \alpha = 0.38. \quad (11)$$

- d) *Arriving β through “Nominal” equation $\alpha + \beta + \gamma = 1$*

$$\beta = 1 - 0.346 - 0.38 \implies \beta = 0.274. \quad (12)$$

Table I, titled “asymmetric factor,” validates counterbalance variables for seizures and normalcy, reducing errors by 32% and increasing detection to 68.375%.

- 2) *S.E Hypothesis 2: Symmetric Localized-Sensor Biased Counter-Balance Ratio Distribution:*

The individual sensors at localized seizure nodes at the wrist are allocated equal priority in this iteration to detect seizures. The subsequent two sensors are considered ancillary to the seizure site. The distribution is symmetrical in the equation representing GTCS, and the nominal values remain unchanged as they represent the totality of seizures experienced throughout the body in both nominal and ictal states

$$\begin{aligned} \text{Principal_equation} &= \sum \text{GTCS} + \text{L_PNES} + \text{R_PNES} \\ &\quad + \text{N_PNES} + \text{Nominal} \\ &= 3.25\alpha + 3.5\beta + 3.25\gamma = 3.2 \quad [\text{Congruent of asymmetric}]. \end{aligned}$$

This establishes that even if the distribution is modified the overall contribution by sensors remain unaffected.

TABLE IV
ASYMMETRIC AND SYMMETRIC FINAL BALANCING FACTORS PER NODE

Node	Symbol	Asymmetric Factor	Symmetric Factor
Ulnar	α	0.346	0.532
Carotid	β	0.274	0.532
Radial	γ	0.034	0.532

- a) *Arriving β :*

$$\begin{aligned} \text{GTCS} - \text{N_PNES} : 0.5\alpha + 0.5\beta + 0.5\gamma \\ = 0.7 - (0.5\alpha + \beta + 0.5\gamma) = 0.6 \\ \text{thus, } \beta = 0.2. \end{aligned} \quad (13)$$

- b) *Arriving subequation γ via β in Principal_equation*

$$\begin{aligned} \text{Principal_equation} &= 3.25\alpha + 3.5 \times 0.2 + 3.25 \\ \gamma &= 0.769 - \alpha(\text{sol2}) \implies \gamma = 3.2. \end{aligned} \quad (14)$$

- c) *Arriving α via backpropagation of $\beta = 0.2$ and $\gamma = 0.769 - \alpha$ in R_PNES*

$$\begin{aligned} 0.25\alpha + 0.5 \times 0.2 + (0.769 - \alpha) &= 0.47 \\ \text{thus, } \alpha &= 0.532. \end{aligned} \quad (15)$$

- d) *Arriving γ through backpropagation to sol 2*

$$\gamma = 0.769 - \alpha \implies \gamma = 0.237. \quad (16)$$

Counterbalance values are validated and displayed in Table I. The variables are added into the Principal equation to evaluate their validity in seizure-related and normal conditions. The error mitigation achieved with sensor counterbalance is 18% higher compared to asymmetric distribution, resulting in an increase in the detection percentile to 95.683%.

Exclusive PNES symptoms encompass limb thrashing, controlled head movements, coherent verbal expression, loss of consciousness, and responsiveness, distinguishing them from GTCS manifestations.

IV. OUR PROPOSED VPSI 2.0 CLASSIFIER

Conventional seizure detection protocols are limited in their ability to accurately classify closely similar ictal symptoms, requiring precise calibration to address patient biomarker variability and system-induced signal irregularities. Detection errors may result in misdiagnosis and delays in therapy administration. The S.E protocol serves as a calibration primitive, balancing FPs and negatives in medical devices. Despite the inherent biomarker noise in epilepsy, S.E-based hardware calibration, as depicted in Fig. 6, incorporating vibration sensors and biomarker recorders, proves useful for identifying erroneous ictal instances in automated seizure detection systems. The S.E concept leverages patient-specific seizure patterns recorded during nonictal phases and calibrated in real-time through the IoMT, offering a vital role in identifying FNs during the patient's ictal phase in PNES cycles. The erratic nature of seizure detection enables S.E to detect error patterns and issue counter-balance variables, relying on offsets created by patient-specific seizure patterns during ictal onset. While exact ictal offsets between patients

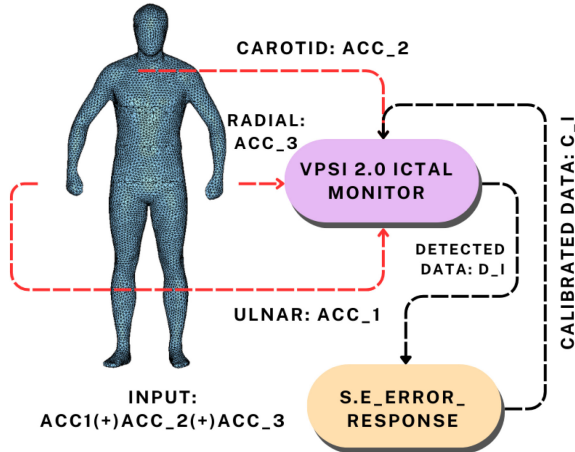


Fig. 4. S.E-based PNES detection optimizer on VPSI 2.0.

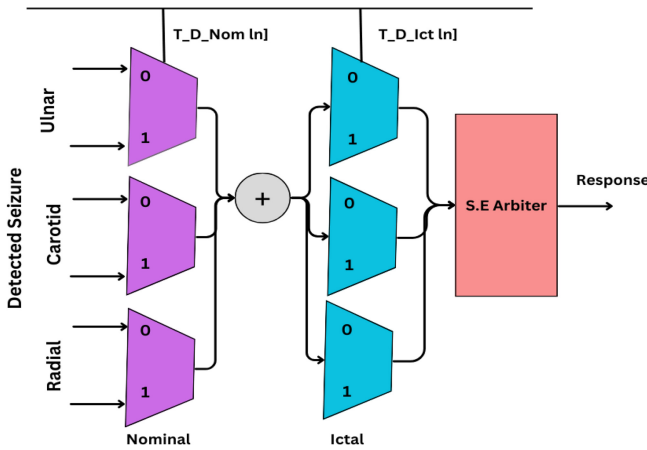


Fig. 5. ASE on VPSI 2.0.

may be challenging to determine, S.E offers a generalized solution for PNES versus GTCSs classification with minimal storage requirements. Consequently, S.E counter-balance presents a promising approach to enhance detection integrity and accuracy in nonclinical seizure monitoring.

A. S.E-VPSI 2.0 Architecture

S.E is useful to generate accurate response/detection and is implemented on an Arduino-based wearable hardware to extract the eccentricities of ictal phase. Arbiter S.E (ASE) is considered where the three nodes generate erratic outcomes and are reconfigured by activating the counter-balance as shown in Figs. 4 and 5. ASE consists of three main components known as calibration factor, node average, and node corroboration factor (NCF). The calibration factor is created with various unpredictable anomalies incurred during ictal phase and the NCF is estimated per sensor failure versus overall expected outcomes. The response is generated by collectively quantifying distinctive detection failures of each node.

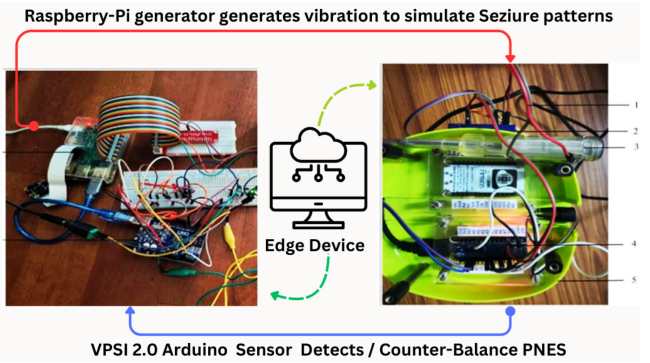


Fig. 6. Experimental testbed: 1) pulse input, 2) pulse sensor, 3) metallic torso prosthesis -1, 4) Arduino nano, and 5) Raspberry Pi housing.

B. Hardware and Software Configuration

To evaluate the proposed VPSI 2.0 classifier framework, we have deployed a real-world rest bed. The test bed consists of two systems: 1) a Raspberry Pi 2 generator that simulates the seizure patterns on a metallic prosthesis and 2) an Arduino nano sensor that houses the S.E-based VPSI 2.0 protocol as shown in Fig. 6.

The Raspberry Pi3, operating Raspbian on 1 GB RAM, integrates with a plastic prosthesis mimicking human torso dimensions. Adjusted by 32 cm for the neck and 15.2 cm for the wrist, the prosthesis meets wrist girth requirements. Seizure detection sites are strategically placed within 85 cm, typical for a 170 cm person's neck-to-wrist span. Vibration patterns from the seizure dataset accurately represent patient status during the ictal phase, while both the Raspberry Pi3 and metallic prosthesis facilitate data sensing. The Arduino® Nano, powered by the ATmega328 microcontroller, offers versatile functionality with 14 digital I/O, eight analog inputs, and six PWM pins, including communication protocols and input voltages of 7–12 V. The prototype's laptop (Intel Core i7-8550u CPU, 16 GB RAM, and 64-bit Windows 10) collects data. The prototype system shows significant potential for accurate seizure detection through advanced sensing and data collection. However, deploying this system on seizure patients requires extensive testing to ensure safety and efficacy. In addition, regulatory approval from the Drugs Controller General of India (DCGI) under the Central Drugs Standard Control Organization (CDSCO) is crucial to ensure adherence to the required standards and regulations prior to clinical implementation.

C. S.E-Based VPSI 2.0 Device Optimization

S.E-based lightweight counter-balance protocol ensures device accuracy. A trusted seizure detection mechanism in the IoMT network is established using the offered economic method. Two phases incorporate counter-balance variables into identified variables in the proposed optimization mechanism: 1) validation and 2) feed-forward.

1) *S.E-Based Validation in VPSI 2.0:* The validation phase occurs concurrently with seizure detection in-house during the ictal phase. Node-specific counterbalances are applied and collected for each detection. Following successful detection,

Algorithm 1 Seizure Detection and Validation

Require: $\alpha, \beta, \gamma, T_D_{Nominal}[n]$,
 $T_D_{Ict}[n], Balances: 0.532(\alpha), 0.2(\beta), 0.237(\gamma)$

Ensure: Decision on the validity of detected seizures

- 1: **for** $k \leftarrow 0$ **to** n **do**
- 2: Calculate Errors: $Err_\alpha[k] \leftarrow |\alpha - T_D_{Nominal}[k]|$ &
 $Err_\beta[k] \leftarrow |\beta - T_D_{Nominal}[k]|$ & $Err_\gamma[k] \leftarrow |\gamma - T_D_{Nominal}[k]|$
- 3: Counterbalance Errors: $Err_\alpha_{bal} \leftarrow Err_\alpha * 0.532$ &
 $Err_\beta_{bal} \leftarrow Err_\beta * 0.2$ & $Err_\gamma_{bal} \leftarrow Err_\gamma * 0.237$
- 4: Bal Err: $Tot_err \leftarrow Err_\alpha_{bal} + \beta_{bal} + \gamma_{bal}$
- 5: Des: $Tot_err[w_in]th_hld?seiz \Rightarrow valid:Declaration \Rightarrow NFR$.
- 6: **end for**

Algorithm 2 Detection Optimization With SGD

Require: $T_D_{Nominal}, T_D_{Ict}, \alpha, \beta, \gamma, lr, batch_size$

Ensure: Decision on the validity of detected seizures

- 1: Initialize ctrn-bal: α, β, γ Define loss_fun:
 $L(\alpha, \beta, \gamma), tot_err, bat_err, mini_bat(trai_data, bat_sz)$
- 2: Err_Cal(data_point, α, β, γ), Tot_Err_Cal(Errors),
Grad_Calc(Errors), validation_data
- 3: **for** epoch in range(num_epochs) of Rand_train_data **do**
- 4: **for** batch in mini_bat(trai_data, bat_sz) **do**
- 5: batch_error = 0
- 6: **for** data_point in batch **do**
- 7: Errors \leftarrow ErrorCalculation(data_point, α, β, γ)
- 8: Grad = $\frac{\partial L}{\partial \alpha}, \frac{\partial L}{\partial \beta}, \frac{\partial L}{\partial \gamma}$ & Tot_Err, Grad \leftarrow Tot_Err_Cal
(Errors), Grad_Calc(Errors)
- 9: **end for**
- 10: Update SGD cnt-bal: $\alpha = \alpha - lr * \frac{\partial L}{\partial \alpha}$ $\beta = \beta - lr * \frac{\partial L}{\partial \beta}$
 $\gamma = \gamma - lr * \frac{\partial L}{\partial \gamma}$
- 11: **end for**
- 12: **end for**

the refined node detections are consolidated by the wearable Arduino processor, as detailed in Algorithm 1.

2) *Feedforward Protocol for VPSI 2.0:* The validation protocols are implemented through a feed-forward mechanism using stochastic gradient descent (SGD) to minimize the loss function during training. Training proceeds over a fixed number of epochs. Within each epoch, the training data is shuffled and divided into mini-batches of a specified size. For each mini-batch (batch_size), the total error and gradients of the loss function with respect to the counter-balance values are computed for each data point. The counter-balance values are then updated using SGD with a fixed learning rate (lr) and the computed gradients. After processing each mini-batch, the average batch error is computed to track training progress. Subsequently, the performance of the updated counter-balance values is validated on a separate dataset to assess generalization. The authentication phase is detailed in Algorithm 2.

V. EXPERIMENTAL RESULTS

The proposed seizure detection technique was validated in 1754 trials on a synthetic prosthesis generating artificially generated ictal profiles from three GTCS and four PNES patients under neurologist supervision. Gait, physical vibrations, pre- and post-ictal investigations, B.P., and heart rate fluctuations were used to create the ictal profile. The model's detection results were tracked and compared to real-time ictal

patterns to ensure accuracy. The simulation uses functional parameters to observe ictal detection false-negatives. A range of conditions were utilized to evaluate the proposed approach across multiple ictal variations in both grand mal and localized epilepsy patterns.

Table II compares our proposed ictal optimization model with state-of-the-art studies. While previous validation relied on one-on-one interviews, our real-time seizure pattern analysis, coupled with hardware security, validates our model for safe detection of GTCS and PNES seizures. The experiment recorded fluctuations in BP and heart rate post-counterbalance. MAP denotes MAP, while SBP, DBP, and HR represent systolic and diastolic B.P., and heart rate, respectively. Where $MAP = DBP + 1/3(SBP - DBP)$. Refer Tables VI and VII. The overall dataset for the experiment carried out can be referred to at <https://archive.org/download/data-comparison-findings-submissionArchive.org> Data Submission.

A. Comparison: S.E Calibrated Detection Outcomes

The system's performance was re-evaluated over 1754 iterations using an asymmetric error balance with alpha set at 0.346, beta at 0.274, and gamma at 0.034. The results showed a 62% increase in accuracy for the ulnar node, a 71.2% increase for the carotid node, and a 68.5% increase for the radial node. The accuracy equation, detailed in (18), involves true positives (TPs), true negatives (TNs), FPs, and FNs

$$\text{Accuracy} = (TP + TN) \div (TP + TN + FP + FN). \quad (17)$$

Retesting with symmetric error balancing led to a positive detection percentile increase of 79.68%, 81.68%, and 80.68% for ulnar, carotid, and radial nodes, respectively.

In the simulation model, ulnar nodes exhibited a failure rate 0.73% higher than comparable nodes. The carotid node outperformed radial and ulnar nodes by 2.5% in GTCS and PNES identification. Housing material vibration dampness significantly affects detection loss. System sensitivity exhibited slight inverse proportionality to augmented protocol calibration oscillation, optimizing FPs and FNs by 58.645%. See Fig. 7, where Sensitivity = $TP \div (TP + FN)$, specificity = $TN \div (TN + FP)$, F-P Rate = $FP \div (TN + FP)$, F-N Rate = $FN \div (TP + FN)$, and F1-score = $2 * TP \div (2 * (TP + FP + FN))$.

The overall improvement factor was assessed for all three nodes against asymmetric localized-sensor biased counter balance ratio distribution outcomes. Symmetric counterbalance yielded a 21.69% enhancement in ulnar node performance compared to asymmetric calibration. In the trials, the carotid node exhibited resilience and responded favorably to the counter-balance methods, closely followed by the radial node. Symmetric counter-balance enhanced carotid sensitivity by 13.84% and radial node sensitivity by 16.39%. Refer Figs. 8–10. The system successfully differentiated between GTCS and PNES with 95.683% accuracy (refer Fig. 11). Fig. 8 illustrates the system's overall sensitivity surpassing each parameter's specificity in the final assessment.

The graphs Figs. 7–9 collectively infer that symmetric error balancing demonstrated a substantial improvement in detection accuracy across all three monitored nodes—ulnar, carotid, and

TABLE V
COMPARISON OF SEIZURE DETECTION RESEARCH WORKS

Research Works	Findings/Implications + Experiment Type	Trials	Automation	Security
Cioriceanu et al.	Older age linked to worse QoL + Interview	Unspecified	No	No
Saker et al.& Newmaster et al	Females show poorer mood in epilepsy Interview	15, 50	No	No
Doss et al.& T. Sawchuk et al.	Patients face education & QoL hurdles + Interview	62, 33	No	No
P.J. Thompson et al. & I. Faiman et al. & C.C. Ogoke et al.	Seizure intensity affects emotional well-being, PNES linked to suicide. + Interview	44 & 2460 & 123	No	No
E. Grillo et al.	Care-givers excel in PNES care + Interview	413	No	No
Current Paper (VPSI 2.0)	Viable model to detect ictals + Wearable prototype	1754	Yes	Yes

TABLE VI
VIBRATION PATTERNS OBSERVED ICTAL STATES

Time	U_yb	C_yb	R_yb	Origin	Referral	Ac_X	Ac_Y
2	S_1	0	0	U_R	S_2	1.71	2
7	S_1	0	0	U_R	NR	2	1.93
4	0	S_2	0	C_D	S_3	1.6	1.87
8	0	S_2	0	C_D	NR	1.83	1.73
6	0	0	S_3	R_D	S_2	1.77	2.33
4	0	0	S_3	R_D	NR	1.73	1.8

TABLE VII
RAW DATA - PERFORMANCE METRICS

Metric	Exp-OP	Ulnar	Carotid	Radial	Overall Deviation
SBP	70	20.3	11.6	23.2	0.74%
DBP	40	11.2	7	14	0.73%
MAP	50	15	9	18	0.72%
HR	58	15.95	8.525	17.05	0.76%
Sensitivity	0.5	0.6	0.4	0.8	-0.2%
Specificity	0.25	0.4	0.325	0.65	-0.84%
F-P Rate	0.5	0.6	0.175	0.35	0.24%
F-N Rate	0.25	0.4	0.125	0.25	-0.04%

radial—associated with seizure classification through B.P. and heart rate monitoring. The graph illustrates the comparative detection performance before and after the application of symmetric error balancing. Prior to this adjustment, detection accuracy was likely hampered by noise and irregularities in the BP and heart rate data. The significant gains observed post-retesting confirm the effectiveness of this approach in refining signal precision and improving the overall reliability of seizure detection. Furthermore, the consistency of the improvement across all three nodes underscores the robustness of the method, reinforcing its potential for widespread clinical application in seizure monitoring.

To further enhance the evaluation of the system's robustness and scalability, 1547 additional tests were performed using a mixed dataset of both nominal and abnormal EEG readings from the Fp1-Ref and Fp2-Ref electrodes, particularly focusing on values exceeding $100 \mu\text{V}$. These tests supplemented the synthetic dataset of 1754 ictal patients, incorporating B.P. and heart rate parameters. By integrating real-world EEG data, the model's generalizability across diverse patient profiles and seizure conditions was rigorously assessed. The results confirmed the system's accuracy and the reliability of the S.E-based counter-balance approach. The supplementary dataset for the experiment carried out can be referred to at <https://archive.org/details/dataset-sampleSupplementary> submission.

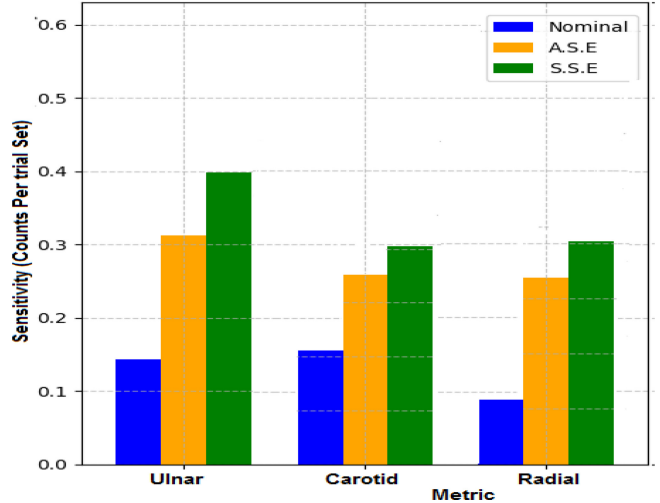


Fig. 7. S.E output: sensitivity comparison of seizure nodes.

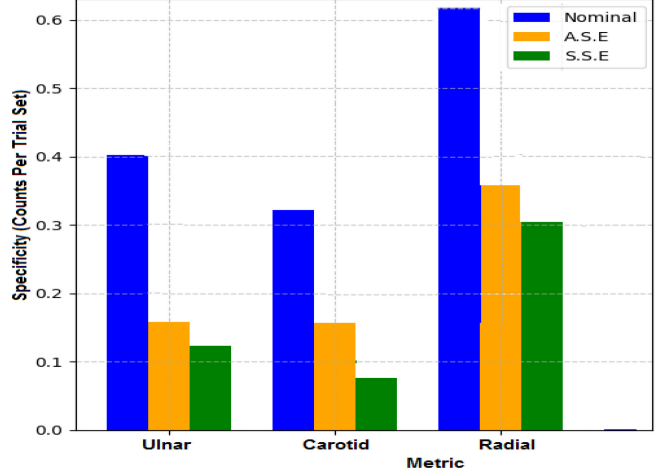


Fig. 8. S output: specificity comparison of seizure nodes.

The current prototype, which operates for approximately 2 h on battery power while processing and transmitting around 2000 raw data entries, establishes a solid foundation for its core functionality. Power management will be addressed in the deployment phase, incorporating duty cycling, local data processing, and energy-efficient communication protocols. This phased approach ensures robust core functionality while optimizing for power consumption, leading to a reliable and efficient final product. The refined design is precise, suitable for chronic seizures, and socially acceptable while worn beneath clothing. This allows seizure patients to use the device

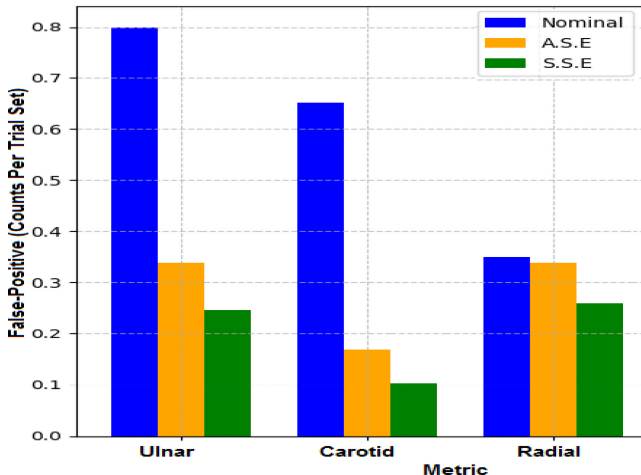


Fig. 9. S.E output: false-positive comparison of seizure nodes.

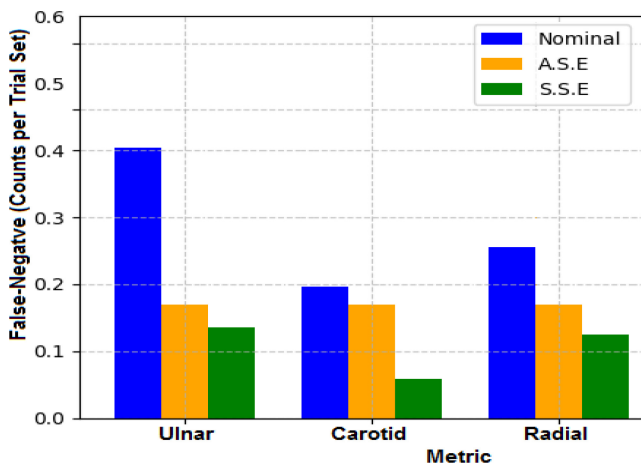


Fig. 10. S.E output: false-negative comparison of seizure nodes.

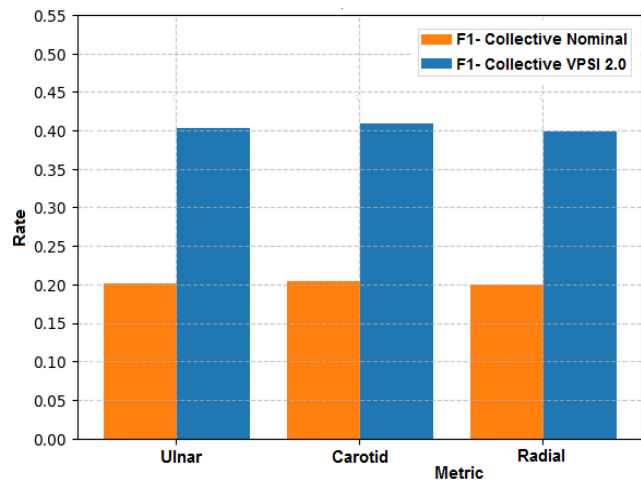


Fig. 11. F1-score before and after VPSI 2.0.

24×7 and maintain independence. Lifestyle choices and preictal symptoms can inform seizure early warning systems for prediction of countermeasures.

VI. CONCLUSION

PNES resemble epilepsy symptoms but lack abnormal brain electrical activity, while seizures stem from psychological distress. A safety addendum addresses distinguishing full-body GTCS seizures from psychiatric origin seizures for reliable automated detection. The IoT-based architecture, which enable real-time, scalable, and remote patient monitoring with continuous data collection, that monitors nerve terminals to autonomously identify convulsions, aided by a peripheral device and wearable Arduino nano processor (to aid compact, customizable, and low-cost solutions for embedded monitoring). The method aims to classify both seizure types, showcasing a prototype with 95.683% failure prevention accuracy. Future research will focus on enhancing accuracy through patient-specific seizure pattern addendum to enhance rotary training of S.E counterbalance protocol. Strict confidentiality and validation using IoT-based medical actuators will further support and refine the approach's efficacy.

REFERENCES

- [1] J. Jungilligens, R. Michaelis, and S. Popkirov, "Misdiagnosis of prolonged psychogenic non-epileptic seizures as status epilepticus: Epidemiology and associated risks," *J. Neurol., Neurosurg. Psy.*, vol. 92, no. 12, pp. 1341–1345, 2021.
- [2] G. Karthikeyan and G. Kousalya, "GTCS-vagus nerve stimulator automation using private IoT-blockchain smartcontract," *Comput. Syst. Eng.*, vol. 44, pp. 1325–1340, Feb. 2023.
- [3] J. M. Stern and N. Salomon, "Vagus nerve stimulator," in *Imaging Epilepsy*. Cham, Switzerland: Springer, 2022, pp. 373–375. [Online]. Available: <https://link.springer.com/book/10.1007/978-3-030-86672-3>
- [4] A. Bozorgi et al., "Significant postictal hypotension: Expanding the spectrum of seizure-induced autonomic dysregulation," *Epilepsia*, vol. 54, no. 9, pp. 127–130, 2013.
- [5] E. Grillo, "Postictal MRI abnormalities and seizure-induced brain injury: Notions to be challenged," *Epilepsy Behav.*, vol. 44, pp. 195–199, Mar. 2015.
- [6] I.-H. Cioriceanu, D. A. Constantin, L. G. Marceanu, C. V. Anastasiu, A. N. Serbanica, and L. Rogozea, "Impact of clinical and socio-demographic factors on Quality of Life in Romanian people with epilepsy," *Healthcare*, vol. 10, no. 10, p. 1909, 2022.
- [7] C. C. Ogoke, W. C. Igwe, and E. N. Umeadi, "Clinical and socio-demographic factors associated with electroencephalographic abnormalities in children with epilepsy," *Annal. Clin. Biomed. Res.*, vol. 2, pp. 35–40, Sep. 2021.
- [8] P. J. Thompson and D. Upton, "The impact of chronic epilepsy on the family," *Seizure*, vol. 1, no. 1, pp. 43–48, 1992.
- [9] I. Faimanet, J. Hodsoll, A. H. Young, and P. Shotbolt, "Increased suicide attempt risk in people with epilepsy in the presence of concurrent psychogenic nonepileptic seizures," *J. Neurol., Neurosurg. Psy.*, vol. 93, no. 8, pp. 895–901, 2022.
- [10] T. S. Saker, M. Katson, S. E. Herskovitz, and M. Herskovitz, "Knowledge and emotional attitudes of health care practitioners regarding patients with psychogenic nonepileptic seizures," *Arquivos de Neuro-Psiquiatria*, vol. 80, no. 11, pp. 1097–1103, 2022.
- [11] J. Doss, "Psychogenic non-epileptic seizures in youth: Individual and family psychiatric characteristics," *Front. Psy.*, vol. 13, Dec. 2022, Art. no. 1068439.
- [12] "The role of IoT in healthcare: Dynamics and significance." 2023. [Online]. Available: <https://onomondo.com/blog/the-role-of-iot-in-healthcare-dynamics-and-significance/>
- [13] T. Sawchuk, J. Buchhalter, and B. Sentf, "Psychogenic non-epileptic seizures in children—psychophysiology & dissociative characteristics," *Psy. Res.*, vol. 294, Dec. 2020, Art. no. 113544.
- [14] K. Newmaster et al., "A review of the multi-systemic complications of a ketogenic diet in infants with epilepsy," *Children*, vol. 9, no. 9, p. 1372, 2022.
- [15] M. S. Nafea and Z. H. Ismail, "Supervised machine learning and Deep Learning techniques for epileptic seizure recognition using EEG signals—A systematic literature review," *Bioengineering*, vol. 9, no. 12, p. 781, 2022.

- [16] D. Zambrana-Vinaroz, J. M. Vicente-Samper, and J. M. Sabater-Navarro, "Validation of continuous monitoring system for epileptic users in outpatient settings," *Sensors*, vol. 22, no. 8, p. 2900, 2022.
- [17] Y.-T. Ng, "Maximizing quality of life in children with epilepsy," *Children*, vol. 10, no. 1, p. 65, 2022.
- [18] R. Caplan, "Cognition and quality of life in children with new-onset epilepsy," *Epilepsy Currents*, vol. 13, no. 2, pp. 85–87, 2013.
- [19] K. Song, J. Fang, L. Zhang, F. Chen, J. Wan, and N. Xiong, "An intelligent epileptic prediction system based on synchrosqueezed wavelet transform and multi-level feature CNN for smart healthcare IoT," *Sensors*, vol. 22, no. 17, p. 6458, 2022.
- [20] A. A. Malibari, "An efficient IOT-artificial intelligence-based disease prediction using lightweight CNN in healthcare system," *Meas., Sensors*, vol. 26, Apr. 2023, Art. no. 100695.
- [21] D. P. Yedurkaret, S. P. Metkar, F. Al-Turjman, T. Stephan, M. Kolhar, and C. Altrjman, "A novel approach for multichannel epileptic seizure classification based on Internet of Things framework using critical spectral verge feature derived from flower pollination algorithm," *Sensors*, vol. 22, no. 23, p. 9302, 2022.
- [22] D. Zambrana-Vinaroz, J. M. Vicente-Samper, J. Manrique-Cordoba, J. M. Sabater-Navarro, "Wearable epileptic seizure prediction system based on machine learning techniques ECG, PPG and EEG Signals," *Sensors*, vol. 22, no. 23, p. 9372, 2022.
- [23] K. K. Dutta, P. Manohar, K. Indira, F. Naaz, M. Lakshminarayanan, and S. Rajagopalan, "Seven epileptic seizure type classification in pre-ictal, ictal and inter-ictal stages using machine learning techniques," *Adv. Mach. Learn. Artif. Intell.*, vol. 4, no. 1, pp. 1–10, 2023.
- [24] M. H. Andarevi and A. A. Iskandar, "A prototype of IOT-based real-time respiratory rate monitoring using an accelerometer sensor," in *Proc. 4th Int. Conf. Biomed. Eng. (IBIOMED)*, 2022, pp. 42–46.
- [25] P. Verma, A. Gupta, M. Kumar, and S. S. Gill, "FCMCPs-COVID: AI propelled fog-cloud inspired scalable medical cyber-physical system, specific to coronavirus disease," *Internet Things*, vol. 23, Oct. 2023, Art. no. 100828.
- [26] P. Bellini, L. A. Ipsaro Palesi, A. Giovannoni, and P. Nesi, "Managing complexity of data models and performance in broker-based Internet/Web of Things architectures," *Internet Things*, vol. 23, Oct. 2023, Art. no. 100834.
- [27] J. Li and Y. Sawano, "The history and innovation of home blood pressure monitors," in *Proc. IEEE Hist. Electrotechnol. Conf. (HISTELCON)*, 2017, pp. 82–86.
- [28] M. Genovese et al., "Safety and efficacy of neurostimulation with a miniaturised vagus nerve stimulation device in patients with multidrug-refractory rheumatoid arthritis: A two-stage multicentre, randomised pilot study," *Lancet Rheumatol.*, vol. 2, pp. e527–e538, Sep. 2020.
- [29] H. Luan and Y. Zhang, "Programmable stimulation and actuation in stretchable electronics," *Adv. Intell. Syst.*, vol. 3, no. 6, 2021, Art. no. 2000228.
- [30] K. Gopalakrishnan, A. Balakrishnan, K. Govardhanan, and S. Selvarasu, "Propositional inference for IOT based dosage calibration system using private patient-specific prescription against fatal dosages," *Sensors*, vol. 23, no. 1, p. 336, 2022.
- [31] M. Qi, Z. Wang, Q. Han, J. Zhang, S. Chen, and Y. Xiang, "Privacy protection for blockchain-based healthcare IoT systems: A survey," *IEEE/CAA J. Automatica Sinica*, vol. 11, no. 8, pp. 1757–1776, 2024.



Karthikeyan Gopalakrishnan received the M.E. and Ph.D. degrees from Anna University, Chennai, India, in 2012 and 2023, respectively.

He is an Assistant Professor with the Department of Computer Science, Coimbatore Institute of Technology (Anna University), Coimbatore, India. Specialization: Application of IoT in seizures.



Arunkumar Balakrishnan received the M.E. and Ph.D. degrees from Anna University, Chennai, India, in 2011 and 2022, respectively.

He is an Assistant Professor with the Department of Computer Science and Engineering, VIT-AP University, Amaravathi, India. Specialization: Cryptography, medical image security, and blockchain.



Kousalya Govardhanan received the M.E. and Ph.D. degrees from Anna University, Chennai, India, in 2001 and 2008, respectively.

Specialization: Cloud computing, AI, and IoT.



Kandala N. V. P. S. Rajesh received the M.Tech. and Ph.D. degrees from Vellore Institute of Technology, Vellore, India, 2013 and 2018, respectively.

He is an Associate Professor with the School of Electronics Engineering, VIT-AP University, Amaravati, India. Specialization: Biomedical signal processing, image processing, and machine and deep learning.